

# Effective Use of GoodingIOD\*

Jim Wright     Bill Chuba  
Analytical Graphics, Inc.

August 30, 2004

## Contents

<b>1</b>	<b>Introduction</b>	<b>2</b>
<b>2</b>	<b>User's Guide</b>	<b>3</b>
2.1	Bring Up the GoodingIOD White Panel . . . . .	3
2.2	Edit the GoodingIOD White Panel . . . . .	4
2.3	Execute the GoodingIOD Program . . . . .	7
2.4	Reduce the Set of Candidate Solutions by Inspection . . . . .	7
2.5	Test Candidate Solutions for the Useful Solution . . . . .	7
2.6	When the Useful Solution is Not Found . . . . .	8
2.7	For Every Candidate Solution . . . . .	8
<b>3</b>	<b>Description of GoodingIOD</b>	<b>8</b>
3.1	Lambert . . . . .	9
3.1.1	Lambert Problem . . . . .	10
3.1.2	Multiple Solutions . . . . .	10
3.1.3	Universal Variables . . . . .	10
3.2	Gooding . . . . .	10
3.2.1	Multiple Solutions . . . . .	11
3.3	A Priori Orbit Information . . . . .	12
3.3.1	For Near-Circular Orbits . . . . .	13
3.3.2	High Eccentricity Orbits . . . . .	14
3.4	White Noise . . . . .	14
3.5	Tropospheric Effects . . . . .	14
3.6	Inspection of Kepler Orbit Element Values . . . . .	15
3.7	Multiple Solutions from Each Set of Distinct Measurement Sets . . . . .	15
3.8	Least Squares . . . . .	15
<b>4</b>	<b>Testing GoodingIOD</b>	<b>16</b>
4.1	Work Summary . . . . .	16
4.1.1	Phase I: Null Tests . . . . .	16
4.1.2	Phase II: White Noise Tests . . . . .	16
4.2	Accuracy Results . . . . .	17
4.2.1	Without White Noise . . . . .	17
4.2.2	With White Noise . . . . .	17
<b>5</b>	<b>Notation and Definitions</b>	<b>20</b>
5.1	Notation . . . . .	20
5.2	Definitions . . . . .	22

---

\*© Analytical Graphics, Inc. 2004

## List of Figures

1	LEO Position Errors Single Station White Noise $\sigma = 10$ arcsec . . . . .	3
2	LEO Velocity Errors Single Station White Noise $\sigma = 10$ arcsec . . . . .	4
3	LEO Position Errors Single Station White Noise $\sigma = 100$ arcsec . . . . .	5
4	LEO Velocity Errors Single Station White Noise $\sigma = 100$ arcsec . . . . .	6
5	LEO Position Errors Single Station with White Noise for $t_3 - t_1 = 8$ min . . . . .	7
6	LEO Velocity Errors Single Station with White Noise for $t_3 - t_1 = 8$ min . . . . .	8
7	LEO Position Errors Single Station White Noise $\sigma = 0.01$ deg . . . . .	9
8	LEO Velocity Errors Single Station White Noise $\sigma = 0.01$ deg . . . . .	10
9	LEO Position Errors Two Stations White Noise $\sigma = 0.01$ deg . . . . .	11
10	LEO Velocity Errors Two Stations White Noise $\sigma = 0.01$ deg . . . . .	12
11	LEO Position Errors Two Stations White Noise $\sigma = 0.01$ deg Full Force Model . . . . .	13
12	LEO Velocity Errors Two Stations White Noise $\sigma = 0.01$ deg Full Force Model . . . . .	14
13	GEO Position Errors Single Station White Noise $\sigma = 2.5$ arcsec . . . . .	15
14	GEO Velocity Errors Single Station White Noise $\sigma = 2.5$ arcsec . . . . .	16
15	GEO Position Errors Single Station White Noise $\sigma = 5$ arcsec . . . . .	17
16	GEO Velocity Errors Single Station White Noise $\sigma = 5$ arcsec . . . . .	18
17	GEO Position Errors Single Station White Noise $\sigma = 10$ arcsec . . . . .	19
18	GEO Position Errors Single Station White Noise $\sigma = 10$ arcsec . . . . .	20
19	GEO Position Errors Multiple Station White Noise $\sigma = 10$ arcsec . . . . .	21

## List of Tables

1	Mean Orbit Period vs Orbit Class . . . . .	12
2	Orbit Period Relations . . . . .	13
3	Notation for Three Times . . . . .	21
4	Notation for Any Common Time . . . . .	22

## 1 Introduction

GoodingIOD<sup>1</sup> (Gooding Initial Orbit Determination) is an algorithm and computer program to estimate the position and velocity of a spacecraft from three pairs of angles measurements and their tracking platform positions. Tracking platforms may be ground stations with tracking sensors or spacecraft with tracking sensors. GoodingIOD was implemented in Version 3.0 of Orbit Determination Tool Kit (ODTK), and is described in Section 3.0 herein. The user will require a basic understanding of GoodingIOD to most effectively use it.

GoodingIOD is similar to other IOD methods only in that its force field is restricted to two-body gravitational dynamics. But full use of two-body dynamics is enabled because, unlike some IOD methods, truncated Taylor's series are not employed. GoodingIOD is further distinguished in that three pairs of angles measurements may be used from one, two, or three distinct tracking platforms. The capability for *multiple platform* IOD has been demonstrated with GoodingIOD, and the dramatic orbit estimation accuracy improvement of double-station IOD over single-station IOD is quantified herein.

Graphics for realistic performance are presented throughout the paper. An associated discussion begins in Section 4.2.2.

Notation and definitions are given in Section 5. ODTK computer data input dialogues have white backgrounds and are referred to as *white panels*. Our use of the term *object* refers to an abstract object, consistent with language used in object oriented programming.

---

<sup>1</sup>See references [2][3][4][5] by Dr. Robert H. Gooding.

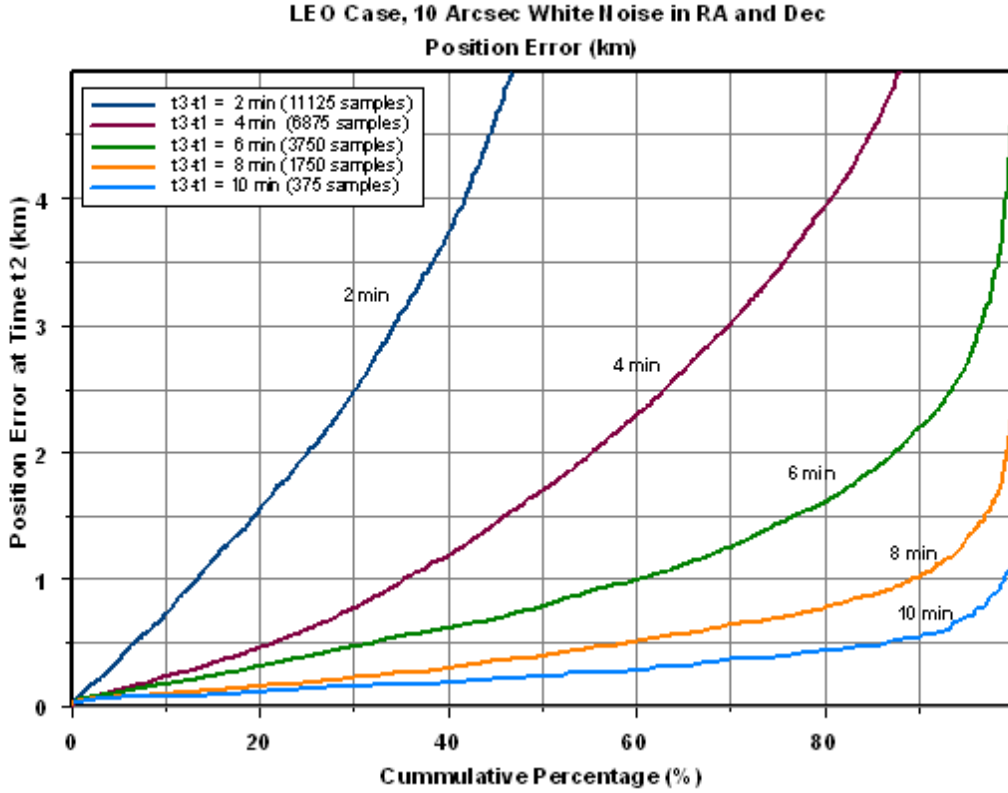


Figure 1: LEO Position Errors Single Station White Noise  $\sigma = 10$  arcsec

## 2 User's Guide

Each applicable pair of angles measurements is one of two types. It consists of right ascension and declination  $(\alpha_j, \delta_j)$  with time tag  $t_j$ , or azimuth and elevation  $(\zeta_j, \eta_j)$  with time tag  $t_j$ , for  $j \in \{1, 2, 3\}$ . The azimuth and elevation measurement platform is ground based, but the right ascension and declination platform may be ground based or space based. Prior to execution of GoodingIOD there must exist at least three distinct pairs of angles measurements  $(\alpha_j, \delta_j)$ , or  $(\zeta_j, \eta_j)$ , with their time-tags  $t_j$  (where  $t_1 < t_2 < t_3$ ), and there must exist the associated platform positions  $\mathbf{s}_j$  from which the angles measurements were generated.

### 2.1 Bring Up the GoodingIOD White Panel

Given a *Scenario* with *Satellite*, *TrackingSystem*, and appropriate angles measurements:

- Select the *Satellite* object from the *Object Browser*
- Insert an *IOD InitialOrbitDetermination* object
- Open the *IOD InitialOrbitDetermination* object from the *Object Browser*
- Change the *HerrickGibbs* default method to *GoodingAnglesOnly*

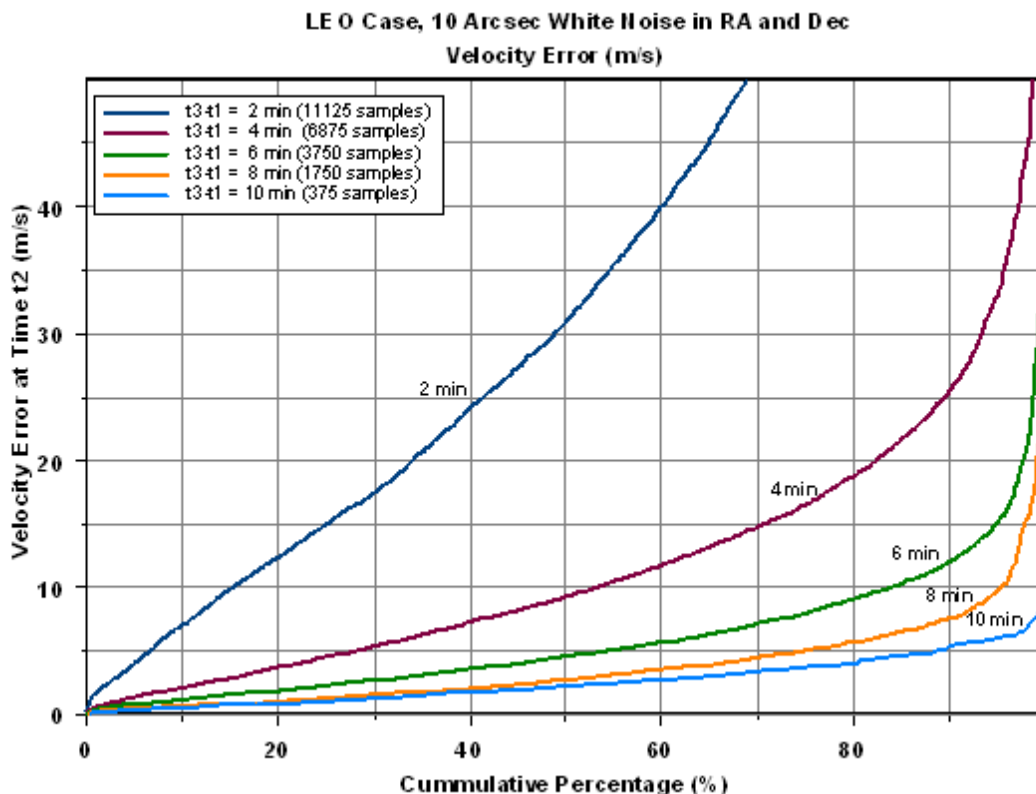


Figure 2: LEO Velocity Errors Single Station White Noise  $\sigma = 10$  arcsec

## 2.2 Edit the GoodingIOD White Panel

The bullet comments in this section are derived, in part, from limited white noise test results. Default values for all *GoodingIOD* white panel fields are presented.

1. Select three pairs of measurement angles (*Items*) with their times  $t_1$ ,  $t_2$ , and  $t_3$  from the existing measurement set.
  - For single-station tracking, the existence of white noise on the angles measurements has a degrading effect on the accuracy of the orbit estimate that becomes worse as times  $t_1$ ,  $t_2$ , and  $t_3$  are more closely spaced; i.e.,  $t_3 - t_1$  must be sufficiently large.
  - For double-station tracking<sup>2</sup>, the orbit estimate errors due to measurement white noise can be significantly reduced when all measurement time-tags are contained within a six minute time interval (LEO), and where  $t_3 - t_1 = 1$  min approximately<sup>3</sup> for each measurement pair.
  - When  $k = 0$ , up to three distinct angles-only IOD solutions normally exist [Gooding[2] p19] for position and velocity. Each solution satisfies two-body accelerations for three distinct pairs of angles measurements. However, at most one of these solutions will satisfy a two-body algorithm consistent with four or more distinct pairs of angles measurements. The user of ODTK requires this solution, so we call this solution the *useful* solution<sup>4</sup>.

<sup>2</sup>Given a tracking system with multiple stations and multiple spacecraft, the use of GoodingIOD for double-station tracking will of course depend on existence of a method to correlate the two tracking station passes a priori.

<sup>3</sup>The case for  $t_3 - t_1 = 1$  min is the only one tested for two-station LEO tracking.

<sup>4</sup>Our definition of *useful* solution refers ultimately to a solution required to initialize an optimal sequential filter. The

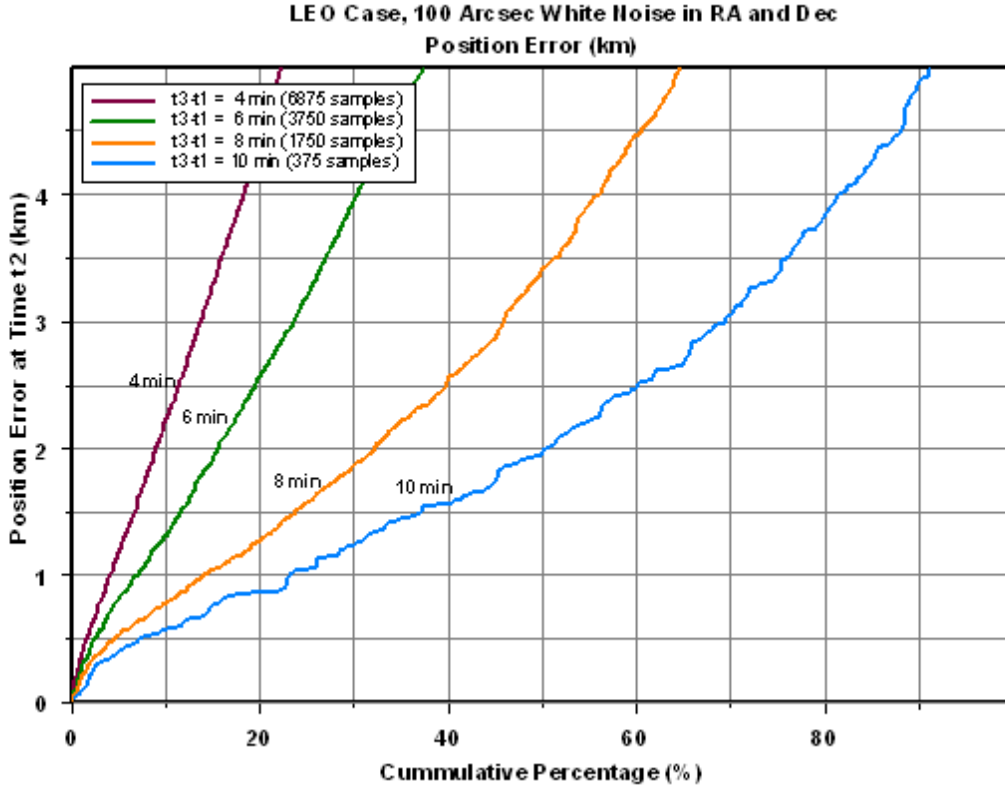


Figure 3: LEO Position Errors Single Station White Noise  $\sigma = 100$  arcsec

- When  $k > 0$  there are usually more than three distinct solutions.
- The number of mathematical orbit solutions, with only one *useful* solution, is increased as the time  $t_3 - t_1$  is increased to enclose more and more half-orbits. This may make the search for the *useful* solution more difficult. Therefore, make  $t_3 - t_1$  as small as practicably possible, keeping in mind that when  $t_3 - t_1$  is too small for single-station tracking, then white noise seriously degrades each orbit estimate.
- For ground station tracking, the three measurement pairs may be selected from different stations, or from different passes from the same station, or from the same station pass. When possible, use the capability for closely spaced measurement time-tags from two-stations to maximize orbit accuracy.
- For ground station azimuth-elevation tracking, avoid low elevations – they have large tropospheric degradations.
- For ground station azimuth-elevation tracking, if measurements are to be selected from within a single ground station pass, find a ground station pass whose maximum elevation is greater than twenty degrees, and select the three measurement pairs symmetrically relative to maximum elevation.

2. Enter a non-negative integer  $HalfRevEstimate = k$  from the set  $\{0, 1, 2, 3, \dots\}$ , default  $k = 0$

GoodingIOD orbit estimate is improved with an overdetermined least squares estimate, and the latter is used to initialize the filter. Apart from this, the mathematician who is interested in finding all solutions that are consistent with three pairs of angles measurements may refer to all solutions as useful.

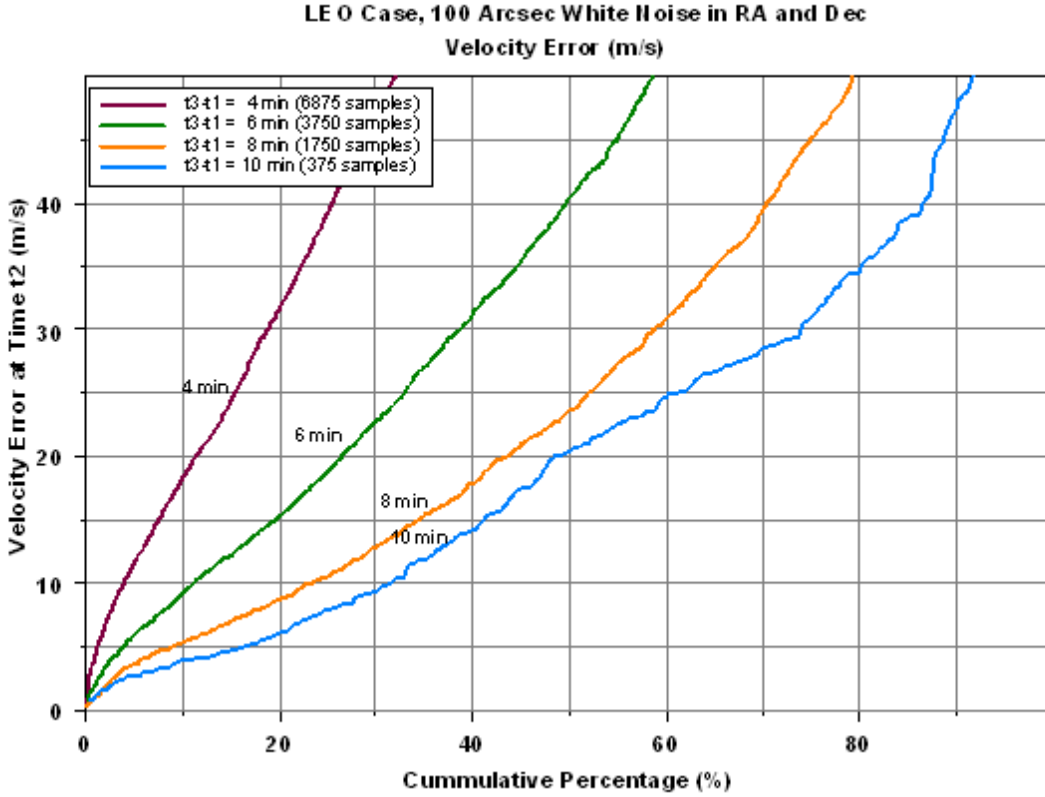


Figure 4: LEO Velocity Errors Single Station White Noise  $\sigma = 100$  arcsec

- Integer  $k$  is the number of half-orbits for which the central angle  $\theta$ , between position vectors  $\mathbf{r}_1$  and  $\mathbf{r}_3$ , is completely contained
  - Integer  $k$  is initially unknown
  - The user should always run GoodingIOD for at least two cases,  $HalfRevEstimate = k$  from the set  $\{0, 1\}$ , when no a priori orbit information is available. This defines a search domain of one orbit in central angle.
  - Integer  $k$  is intimately related to selection of measurement angles pairs. See Section 3 below for help in selecting a value for  $k$
3. Bear in mind the default values for  $Range1Estimate = \rho_1^{(0)}$  and  $Range3Estimate = \rho_3^{(0)}$ .
- It may be necessary to modify the default initial values  $Range1Estimate = \rho_1^{(0)} = 5$  er and  $Range3Estimate = \rho_3^{(0)} = 5$  er in order to find the useful solution; e.g., for LEO we know that  $\rho_1 < 1.0$  er and  $\rho_3 < 1.0$  er, so try  $\rho_1^{(0)} = \rho_3^{(0)} = 0.5$  er. Default values for  $\rho_1^{(0)}$  and  $\rho_3^{(0)}$  are inaccurate first guesses, necessarily. They are used in iterative calculations to find accurate estimates of  $\rho_1$  and  $\rho_3$ , associated with a solution for some orbit estimate. When that orbit estimate is *useful*, then the default values for  $\rho_1^{(0)}$  and  $\rho_3^{(0)}$  have served their purpose. When the orbit estimate is not useful, and all multiple solutions have been examined and determined not useful, it will be necessary to modify the initial values  $\rho_1^{(0)}$  and  $\rho_3^{(0)}$  in a search for a useful orbit estimate.
  - See Section 3 below for help in selecting values for  $\rho_1^{(0)}$  and  $\rho_3^{(0)}$

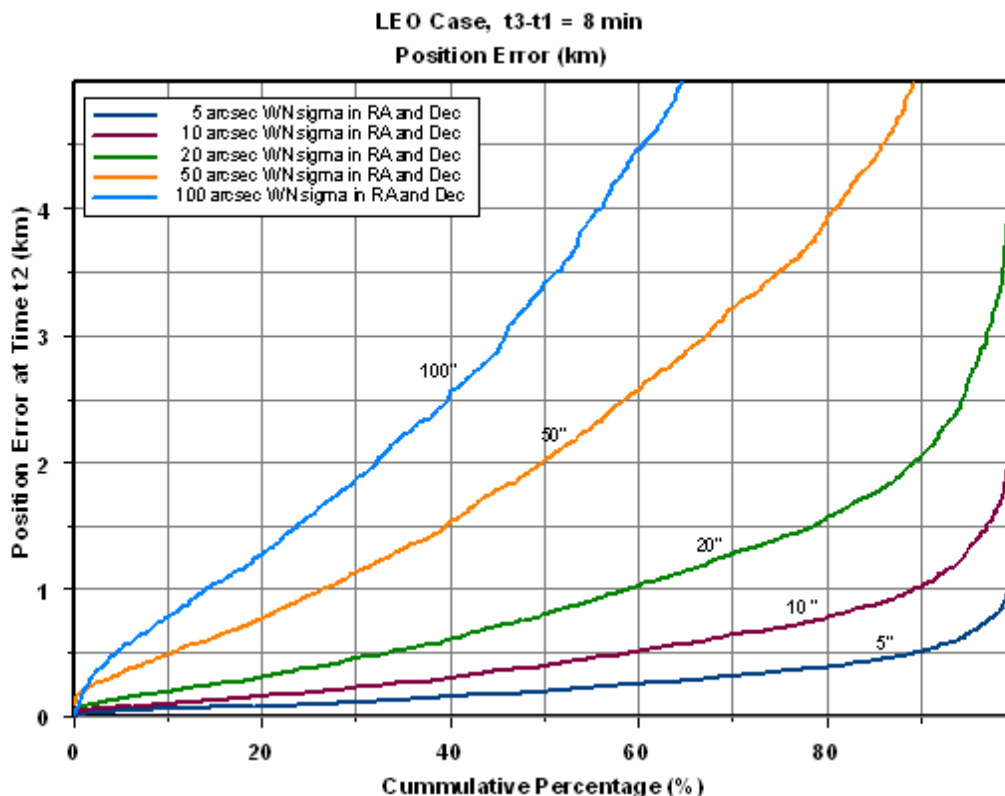


Figure 5: LEO Position Errors Single Station with White Noise for  $t_3 - t_1 = 8$  min

### 2.3 Execute the GoodingIOD Program

1. Execute GoodingIOD
2. Zero, one, or multiple candidate solutions will be calculated

### 2.4 Reduce the Set of Candidate Solutions by Inspection

Given one or more candidate solutions, then for each solution:

1. Change the *OrbitState* from *Cartesian* to *Keplerian*
2. Inspect the Keplerian orbit values and, for multiple solutions, discard those solutions for which values of  $a$  and/or  $e$  are unlikely based on a priori knowledge

### 2.5 Test Candidate Solutions for the Useful Solution

Given multiple candidate solutions remaining, test each solution by running iterative least squares on it with more than three pairs of angles measurements. Discard each solution that iteratively diverges in least squares. Least squares will converge only on the useful solution, and will generate a significantly improved orbit estimate, ready for seeding the optimal sequential filter.

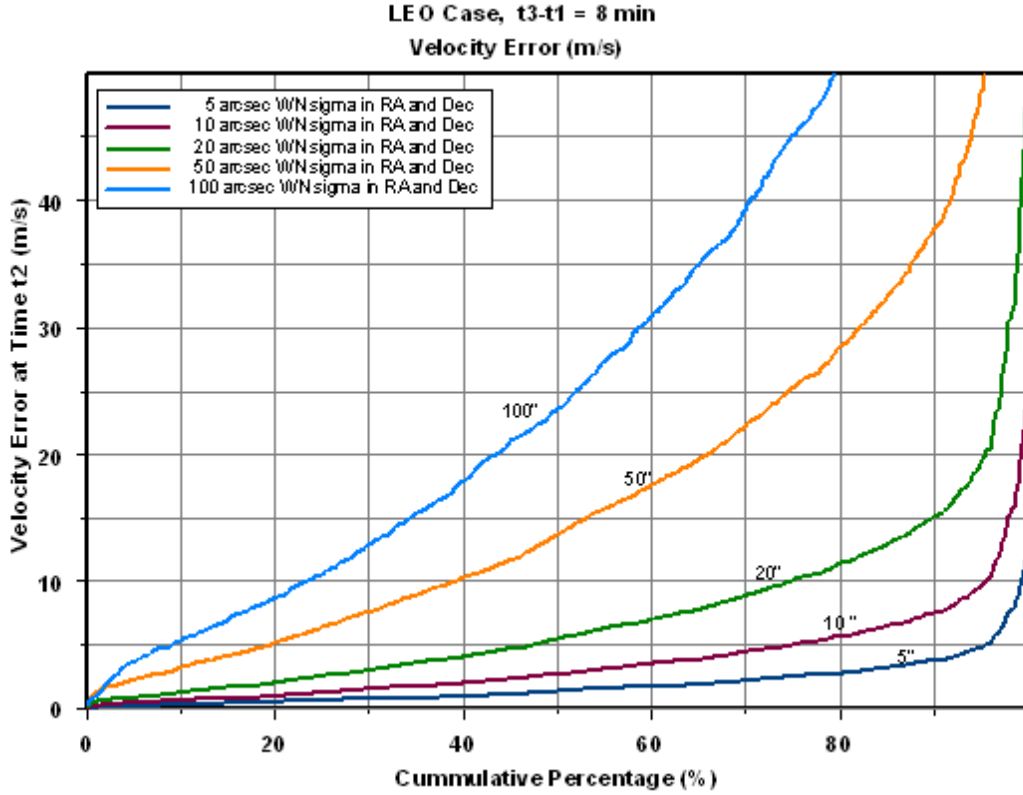


Figure 6: LEO Velocity Errors Single Station with White Noise for  $t_3 - t_1 = 8$  min

## 2.6 When the Useful Solution is Not Found

For any measurement set that does not immediately yield a useful solution, one should select three different pairs of measurement angles, and try again. The useful solution may be difficult to find if:

- the measurement set is physically singular, or nearly so; e.g., the ground station position vector is contained in the plane of the orbit
- the default values for  $\rho_1^{(0)}$  and  $\rho_3^{(0)}$  are inappropriate
- the user is unlucky enough to initially select three sets of angles measurements where the first and third measurements span a central angle that is very close to  $N\pi$ ,  $N \in \{1, 2, 3, \dots\}$

## 2.7 For Every Candidate Solution

Run least squares on every candidate GoodingIOD solution, using an overdetermined set of angles measurements. This will confirm (or deny) that the candidate solution is a useful solution. If confirmed, least squares will generate a significantly improved orbit estimate, ready for seeding the optimal sequential filter.

## 3 Description of GoodingIOD

Given tracking platform positions, GoodingIOD calculates orbit solutions that complete the first and third unit range vectors for which pairs of angles are known but ranges are missing. From each such solution the inertial components of position and velocity are automatically implied.



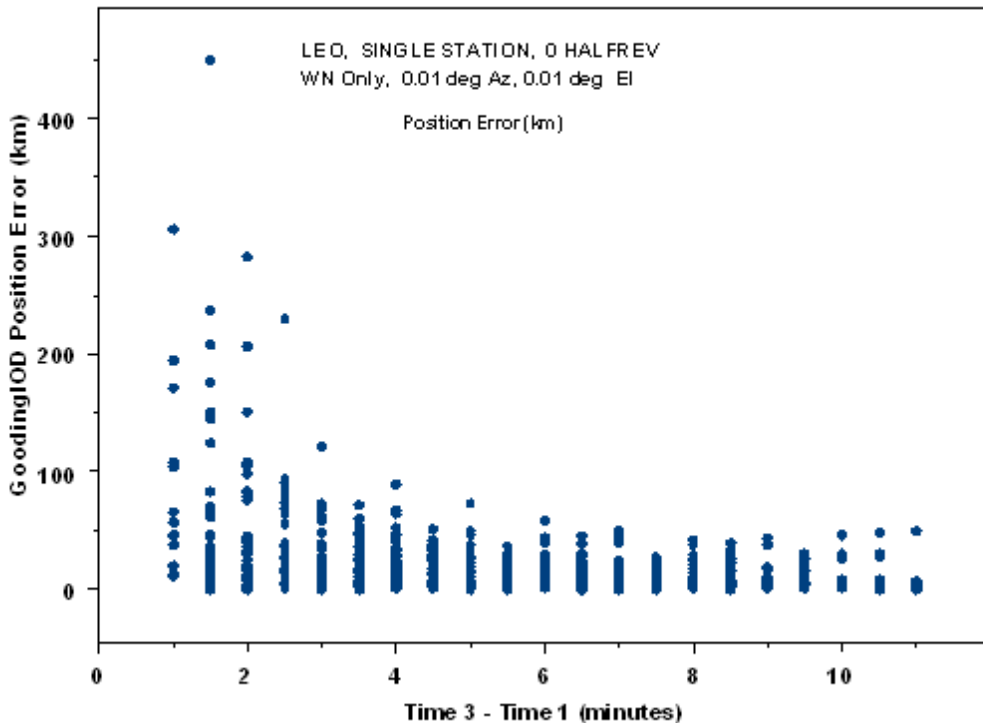


Figure 7: LEO Position Errors Single Station White Noise  $\sigma = 0.01$  deg

Components of unambiguous unit range vector estimates  $\mathbf{L}_1$ ,  $\mathbf{L}_2$  and  $\mathbf{L}_3$  are calculated directly from measured angles pairs at times  $t_1$ ,  $t_2$ , and  $t_3$ . Unit vectors  $\mathbf{L}_j$ ,  $j \in \{1, 2, 3\}$ , are accurate three-dimensional direction pointers from tracking platform to spacecraft, but values for the lengths (ranges)  $\rho_j$  of the range vectors  $\boldsymbol{\rho}_j = \rho_j \mathbf{L}_j$  are unknown. Initial guesses  $\rho_1^{(0)}$  and  $\rho_3^{(0)}$  are defined by the user, or by program default. Vectors  $\mathbf{L}_1$  and  $\mathbf{L}_3$  are then multiplied by initial range value guesses  $\rho_1^{(0)}$  and  $\rho_3^{(0)}$  respectively to derive range vector estimates  $\boldsymbol{\rho}_1^{(0)}$  and  $\boldsymbol{\rho}_3^{(0)}$  at times  $t_1$  and  $t_3$ . Vectors  $\boldsymbol{\rho}_1^{(0)}$  and  $\boldsymbol{\rho}_3^{(0)}$  are correctly directed, but their length estimates may be poor. Vectors  $\boldsymbol{\rho}_1^{(0)}$  and  $\boldsymbol{\rho}_3^{(0)}$  are added to known and accurate platform position vectors  $\mathbf{s}_1$  and  $\mathbf{s}_3$  respectively at times  $t_1$  and  $t_3$  to provide spacecraft position vector estimates  $\mathbf{r}_1^{(0)} = \mathbf{s}_1 + \boldsymbol{\rho}_1^{(0)}$  and  $\mathbf{r}_3^{(0)} = \mathbf{s}_3 + \boldsymbol{\rho}_3^{(0)}$  at times  $t_1$  and  $t_3$ . Errors in the spacecraft position vector estimates  $\mathbf{r}_1^{(0)}$  and  $\mathbf{r}_3^{(0)}$  may be large, in both direction and size. Even so, we have two spacecraft position vector estimates  $\mathbf{r}_1^{(0)}$  and  $\mathbf{r}_3^{(0)}$  at two distinct times  $t_1$  and  $t_3$ .

### 3.1 Lambert

The unknown central angle  $\theta$  between true position vectors  $\mathbf{r}_1$  and  $\mathbf{r}_3$ , in the plane of  $\mathbf{r}_1$  and  $\mathbf{r}_3$ , is related to the orbit period  $P$ , and measurement time-tag difference  $(t_3 - t_1)$ . For each value of  $\theta$ , and for integers  $k \in \{0, 1, 2, 3, \dots\}$ , define  $k$  such that  $(k)\pi < \theta \leq (k+1)\pi$ .

Examples: When  $0 < \theta \leq \pi$ , then  $k = 0$ , and the central angle  $\theta$  is completely contained within the first one-half orbit. When  $\pi < \theta \leq 2\pi$ , then  $k = 1$ , and the central angle  $\theta$  is completely contained within one orbit. Thus  $k$  is the number of half-orbits for which the central angle  $\theta$ , between position vectors  $\mathbf{r}_1$  and  $\mathbf{r}_3$ , is completely contained. When the orbit is circular, the relation between  $(t_3 - t_1)$ , orbit period  $P$ , and  $k$  is

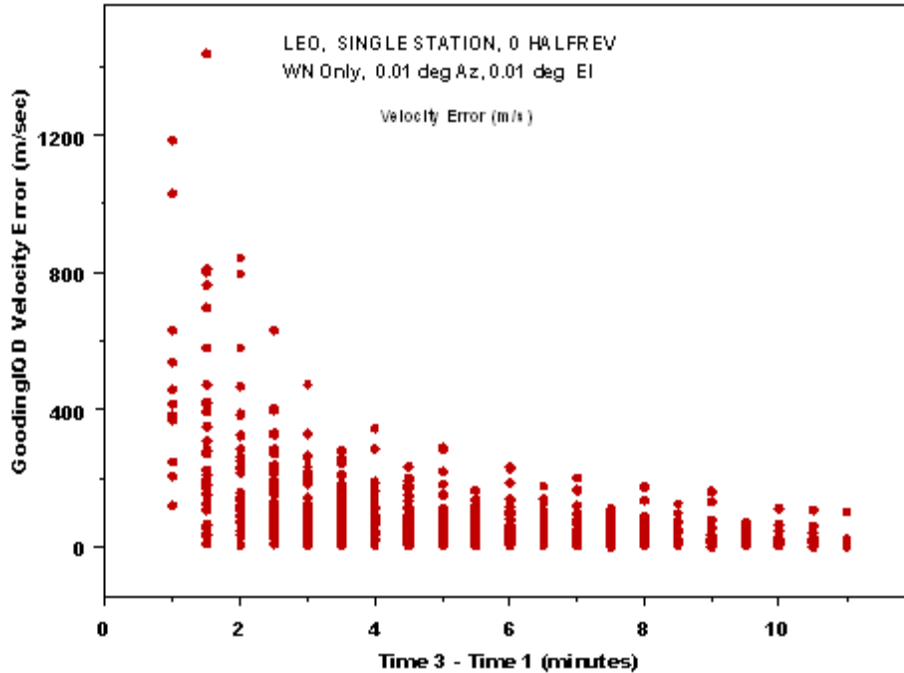


Figure 8: LEO Velocity Errors Single Station White Noise  $\sigma = 0.01$  deg

simple, and the user can make a good guess for  $k$  (see Table 2). But when the orbit is highly eccentric, this relation is not obvious.

### 3.1.1 Lambert Problem

Given values for components of any two distinct spacecraft position vectors  $\mathbf{r}_1$  and  $\mathbf{r}_3$ , and their times  $t_1$  and  $t_3$ , calculate the spacecraft velocity  $\dot{\mathbf{r}}_1$  at time  $t_1$ , or calculate the spacecraft velocity  $\dot{\mathbf{r}}_3$  at time  $t_3$ .

### 3.1.2 Multiple Solutions

When  $k = 0$  or  $k = 1$ , Lambert's Problem has exactly one solution, but when  $k \geq 2$ , Lambert's Problem, like a quadratic equation, has two solutions, no solution, or one solution in a limiting case that occurs with probability zero. Indicator  $i = 0$  if  $k \in \{0, 1\}$ , but  $i \in \{0, 1\}$  if  $k \geq 2$ . This Indicates which of two Lambert solutions are to be used, if there are two.

### 3.1.3 Universal Variables

Gooding's implementation of the Lambert Problem solution is an accurate, two-iteration universal one, valid for all conic orbits: ellipse, parabola, and hyperbola.

## 3.2 Gooding

The GoodingIOD algorithm submits  $\mathbf{r}_1^{(0)}$  and  $\mathbf{r}_3^{(0)}$ , with times  $t_1$  and  $t_3$ , to the Lambert algorithm to calculate velocity  $\dot{\mathbf{r}}_1^{(0)}$ . Although the velocity vector  $\dot{\mathbf{r}}_1^{(0)}$  is likely a poor estimate of  $\dot{\mathbf{r}}_1$ , at least we have a complete orbit estimate from  $\mathbf{r}_1^{(0)}$  and  $\dot{\mathbf{r}}_1^{(0)}$ . This enables the propagation of  $\mathbf{r}_1^{(0)}$  and  $\dot{\mathbf{r}}_1^{(0)}$  to time  $t_2$  to obtain estimates

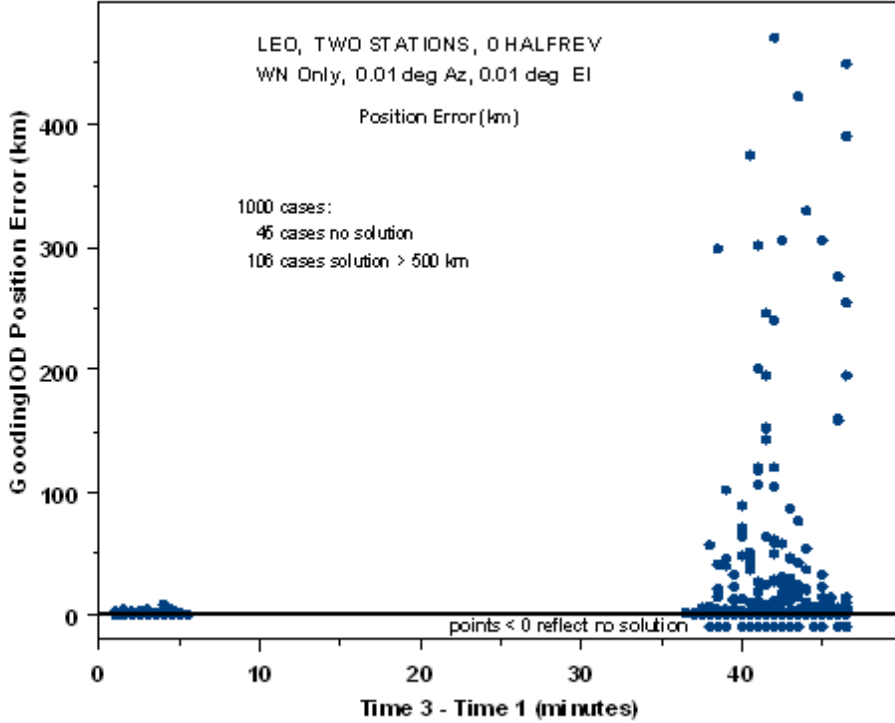


Figure 9: LEO Position Errors Two Stations White Noise  $\sigma = 0.01$  deg

$\mathbf{r}_2^{(0)}$  (and  $\dot{\mathbf{r}}_2^{(0)}$ ). Calculate  $\boldsymbol{\rho}_2^{(0)} = \mathbf{r}_2^{(0)} - \mathbf{s}_2$ , an erroneous estimate of the true range vector  $\boldsymbol{\rho}_2$ . Recall that  $\mathbf{L}_2$  (from angles data) is a good estimate of the unit range vector at time  $t_2$ , so project  $\boldsymbol{\rho}_2^{(0)}$  onto a plane orthogonal to  $\mathbf{L}_2$  to define two components of the error in  $\boldsymbol{\rho}_2^{(0)}$ . Now correct  $\rho_1^{(0)}$  and  $\rho_3^{(0)}$  to reduce the two components of error in  $\boldsymbol{\rho}_2^{(0)}$ , and generate improved estimates  $\rho_1^{(1)}$  and  $\rho_3^{(1)}$  of range, thereby also calculating improved estimates  $\mathbf{r}_1^{(1)}$  and  $\dot{\mathbf{r}}_1^{(1)}$  of position and velocity. This procedure is iterated on integer  $i$  so as to drive the two components of error in  $\boldsymbol{\rho}_2^{(i)}$  to zero, thereby deriving best estimates of  $\rho_1$ ,  $\rho_3$ ,  $\mathbf{r}_2$ , and  $\dot{\mathbf{r}}_2$ .

When the embedded Lambert algorithm provides a solution for the spacecraft velocity  $\dot{\mathbf{r}}_1$  at time  $t_1$ , then GoodingIOD converges to a *local* solution for  $\mathbf{r}_2$  and  $\dot{\mathbf{r}}_2$ . But the price for extraordinary initial errors in  $\rho_1^{(0)}$  and  $\rho_3^{(0)}$  is that the *local* solution for  $\mathbf{r}_2$  and  $\dot{\mathbf{r}}_2$  may not be useful.

### 3.2.1 Multiple Solutions

When  $k = 0$ , there do formally exist either 0, 1, 2, or 3 distinct solutions to the GoodingIOD problem. Unfortunately, there is no sure technique to identify the number of distinct solutions a priori. When there are 2 or 3 distinct solutions, only one of them is useful, but we have found that in the large majority of cases tested, that one is found. When there are formally 3 distinct solutions, two of them may be complex, and will not be found, because the algorithm is restricted to the real domain.

As  $k$  is increased, the number of solutions also increases, though only up to some maximum value. If the value of  $k$  is not known in advance, therefore, the search for the useful solution can get increasingly complicated.

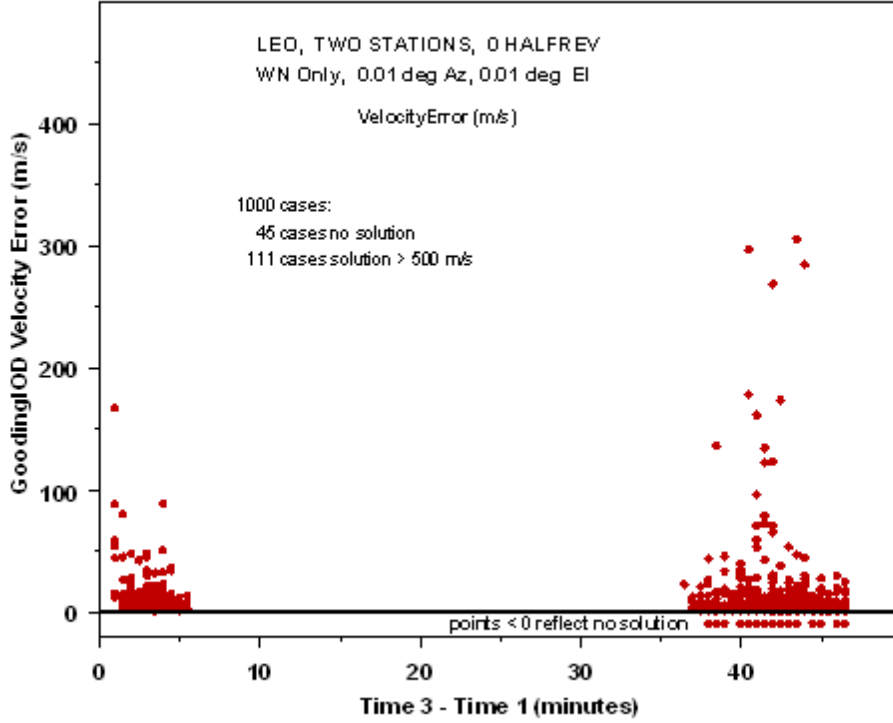


Figure 10: LEO Velocity Errors Two Stations White Noise  $\sigma = 0.01$  deg

### 3.3 A Priori Orbit Information

When there are multiple distinct solutions, only one of them will be useful – associated with the true orbit. It is necessary to correctly couple the selections of the three measurement pair time-tags  $t_1$ ,  $t_2$ , and  $t_3$  with the *HalfRevEstimate* =  $k$  from the set  $\{0, 1, 2, 3, \dots\}$  in order to find the useful solution. One way to do this is to search through  $k \in \{0, 1, 2, 3, \dots\}$  beginning with  $k = 0$ . But when the user has useful a priori information (e.g., orbit class LEO, MEO, GEO, HEO, orbit period  $P$ , semi-major axis  $a$ , or eccentricity  $e$ ), then the search for the useful solution may be simplified. Table 1 correlates orbit class roughly with  $P$  (min),  $P$  (sec),  $a$  (km), and  $e$ .

Orbit Class	$P$ (min)	$P$ (sec)	$a$ (km)	$e$
LEO	100	6000	7137	$0.000 < e < 0.050$
GEO	1436	86169	42163	$0.000 < e < 0.001$
GPS (MEO)	718	43080	26560	$0.000 < e < 0.001$
HEO	718	43080	26561	0.7 (Molniya)

Table 1: Mean Orbit Period vs Orbit Class

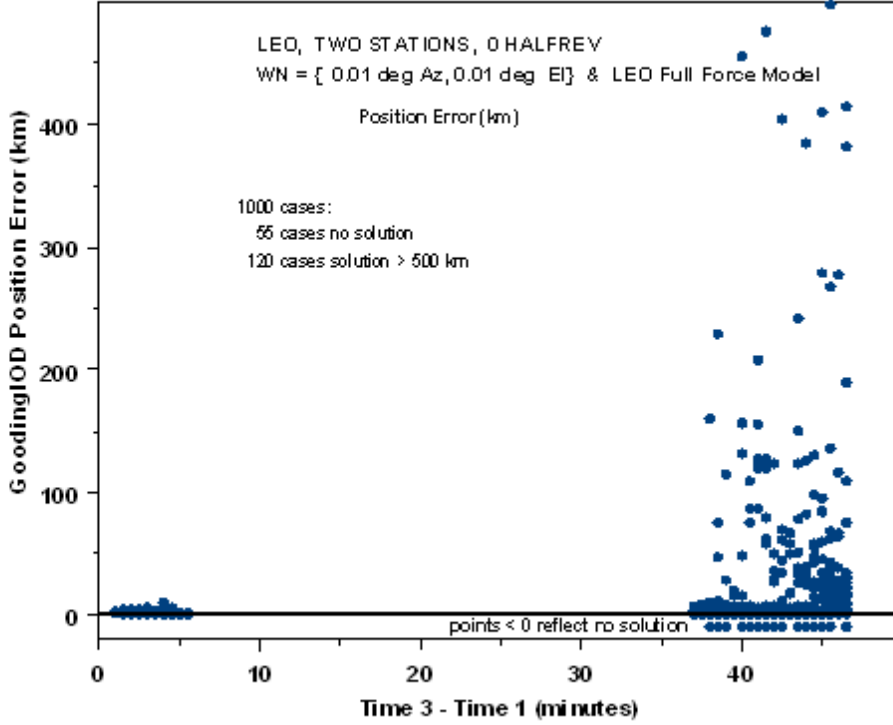


Figure 11: LEO Position Errors Two Stations White Noise  $\sigma = 0.01$  deg Full Force Model

### 3.3.1 For Near-Circular Orbits

With eccentricity zero (or near zero), any uniform partition of orbit period  $P$  maps uniformly (or almost uniformly) to increments in central angle – true argument of latitude differences. This enables association of orbit period  $P$  with the measurement time-tag difference  $t_3 - t_1$  and the *HalfRevEstimate* =  $k$ . For single-station IOD<sup>5</sup>, the simplest approach is to choose  $k = 0$ , then select measurements such that  $0 < t_3 - t_1 < P/2$ , but such that as much of the interval  $[t_1, t_3]$  is used as possible in this selection so as to attenuate the effects of measurement white noise. Table 2 correlates  $k$  with  $P$  and  $t_3 - t_1$ .

$t_3 - t_1$ vs $P$	$k$
$0 < t_3 - t_1 < P/2$	0
$P/2 < t_3 - t_1 < P$	1
$P < t_3 - t_1 < (3/2)P$	2
$(3/2)P < t_3 - t_1 < 2P$	3
$\vdots$	$\vdots$

Table 2: Orbit Period Relations

<sup>5</sup>Double-station IOD is preferred for accuracy.

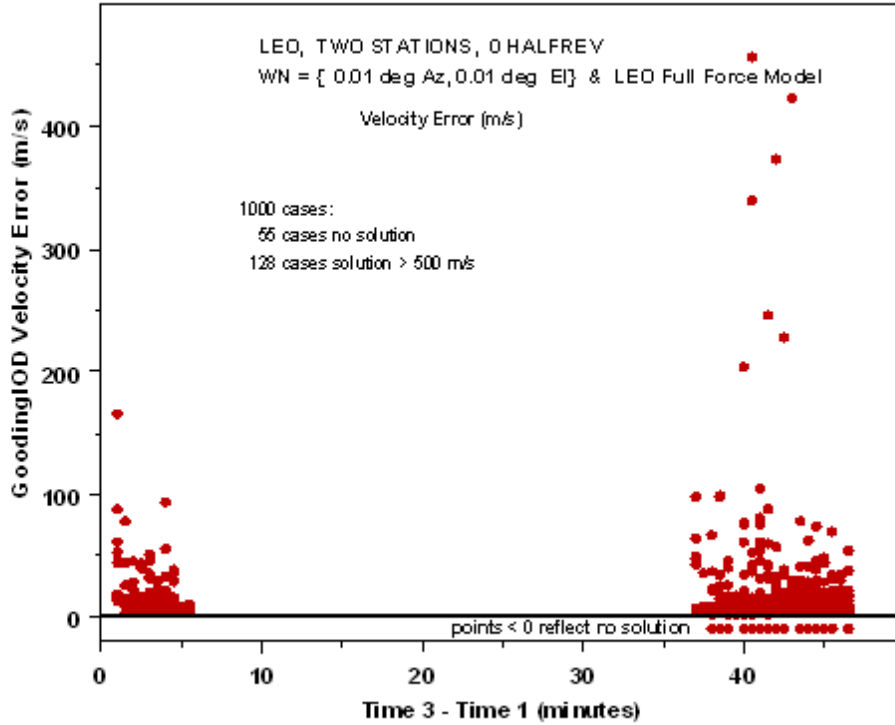


Figure 12: LEO Velocity Errors Two Stations White Noise  $\sigma = 0.01$  deg Full Force Model

### 3.3.2 High Eccentricity Orbits

Given an a priori estimate for orbit period  $P$ , and knowing that the eccentricity  $e$  is large (e.g.,  $e > 0.7$ ), one may choose time-tags  $t_1$ ,  $t_2$ , and  $t_3$  such that  $0 < t_3 - t_1 < P$ . Then one must perform two sets of tests with  $HalfRevEstimate = k$ , for  $k = 0$ , and for  $k = 1$ .

### 3.4 White Noise

Gauss[1] discovered white noise<sup>6</sup> on telescopic angles measurements in right ascension and declination in 1795, while performing orbit determination. All real angles measurements have white noise that degrades all algorithms<sup>7</sup> for angles-only IOD. For single-station single-pass LEO tracking GoodingIOD overcomes the white-noise problem when  $t_3 - t_1 > 0$  is sufficiently large. For two-station LEO tracking, GoodingIOD significantly reduces position and velocity errors due to white-noise, relative to single-station tracking, if all measurements are selected from a common six minute time interval and  $t_3 - t_1 = 1$  min approximately.

### 3.5 Tropospheric Effects

Degrading effects of the troposphere, from ground based platforms, can be significantly reduced by selecting measurements whose elevations are greater than 10 deg.

<sup>6</sup>Gauss[1] invoked the normal density function to model white noise, and invented the iterative least squares algorithm (1795) to perform orbit determination on an overdetermined set of telescopic measurements in right ascension and declination.

<sup>7</sup>The classical LaPlace IOD method is destroyed by white noise if its RMS is significant, when applied to geocentric orbits .

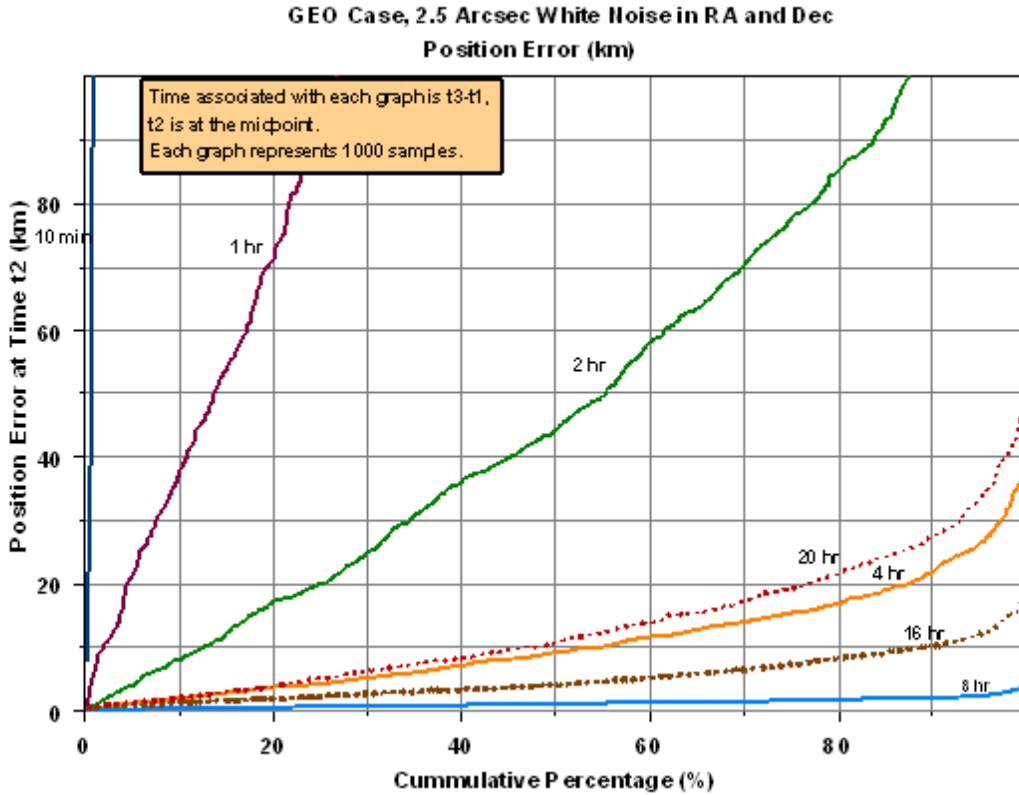


Figure 13: GEO Position Errors Single Station White Noise  $\sigma = 2.5$  arcsec

### 3.6 Inspection of Kepler Orbit Element Values

Given a priori information regarding the orbit, and given multiple solutions from the same measurement set, the user can frequently eliminate useless solutions by inspection of the Kepler orbit elements, particularly the semi-major axis and eccentricity.

### 3.7 Multiple Solutions from Each Set of Distinct Measurement Sets

Comparison of sets of multiple solutions from distinct measurement sets may, or may not, identify the useful solution.

### 3.8 Least Squares

Given multiple solutions from the same measurement set, the user can test each solution by running least squares on it with an overdetermined set (more than three) of angles measurements. Least squares will converge only on the useful solution.

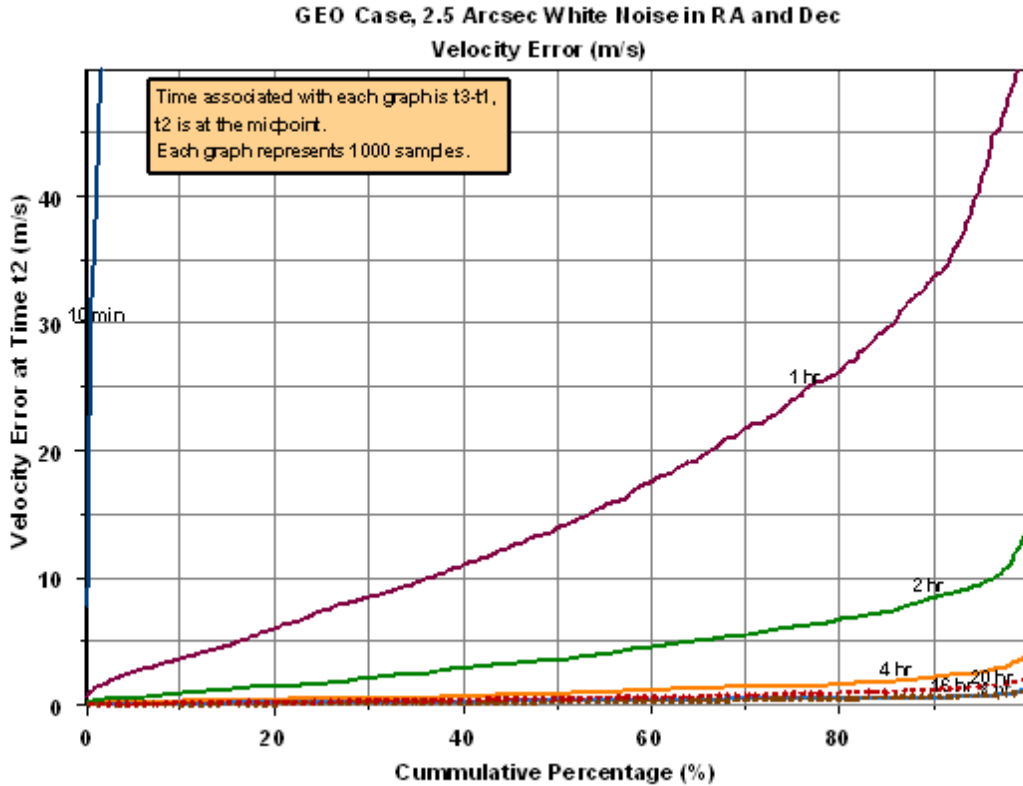


Figure 14: GEO Velocity Errors Single Station White Noise  $\sigma = 2.5$  arcsec

## 4 Testing GoodingIOD

### 4.1 Work Summary

#### 4.1.1 Phase I: Null Tests

The first phase was designed to test GoodingIOD according to its designed hypotheses:

- Two-body geopotential gravity model
- No force modeling errors
- No white noise on angles measurements

The first phase required the development and processing of simulated angles data without white noise on the angles data and without acceleration perturbations in the orbit propagator; i.e., a two-body gravitational field was used to define accelerations. These test cases are referred to as *null* test cases. Our purpose here was to validate our version of GoodingIOD according to its designed hypotheses.

GoodingIOD was null tested and validated with simulated azimuth and elevation angles data, unperturbed by white noise, during a six month Phase I testing interval with Bob Gooding.

#### 4.1.2 Phase II: White Noise Tests

The second phase was designed to test GoodingIOD on its response to realistic white noise on angles measurements. From experience, we know that all angles tracking measurements contain white noise sequences. Azimuth and elevation measurements and right ascension and declination measurements, inclusive of Gaussian



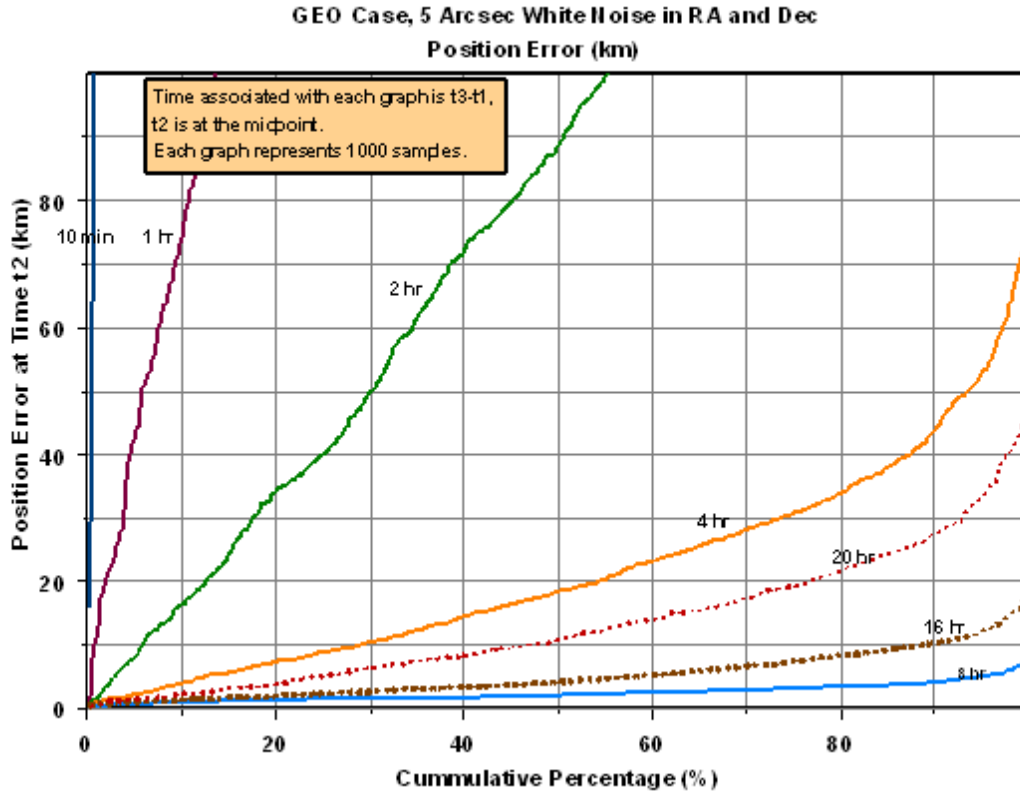


Figure 15: GEO Position Errors Single Station White Noise  $\sigma = 5$  arcsec

white noise, were simulated for LEO, GEO, and HEO cases. The simulated data were used to perform orbit determination with GoodingIOD.

**Acceptance Criterion** The performance of GoodingIOD, on three pairs of realistic angles measurements tracking geocentric spacecraft, is defined to be acceptable when its output estimate of position and velocity can be used successfully to seed a least squares orbit determination (LSOD) on an overdetermined set (more than three measurement pairs) of measurements, where the LSOD uses a full force model.

## 4.2 Accuracy Results

### 4.2.1 Without White Noise

With two-body gravitational dynamics, the absence of measurement modeling errors and force modeling errors, on simulated angles tracking data for null test cases, GoodingIOD performed as expected by Bob Gooding. The AGI version was validated according to its designed hypotheses.

### 4.2.2 With White Noise

GoodingIOD white noise accuracy results are displayed graphically herein. It is expected that the *Acceptance Criterion* defined above will be met for more than 90% (TBD) of experimental attempts, when performed by experienced users.

All figures reflect the use of two-body dynamics in the simulations except for Figs. 11 and 12; full force model dynamics were used here.

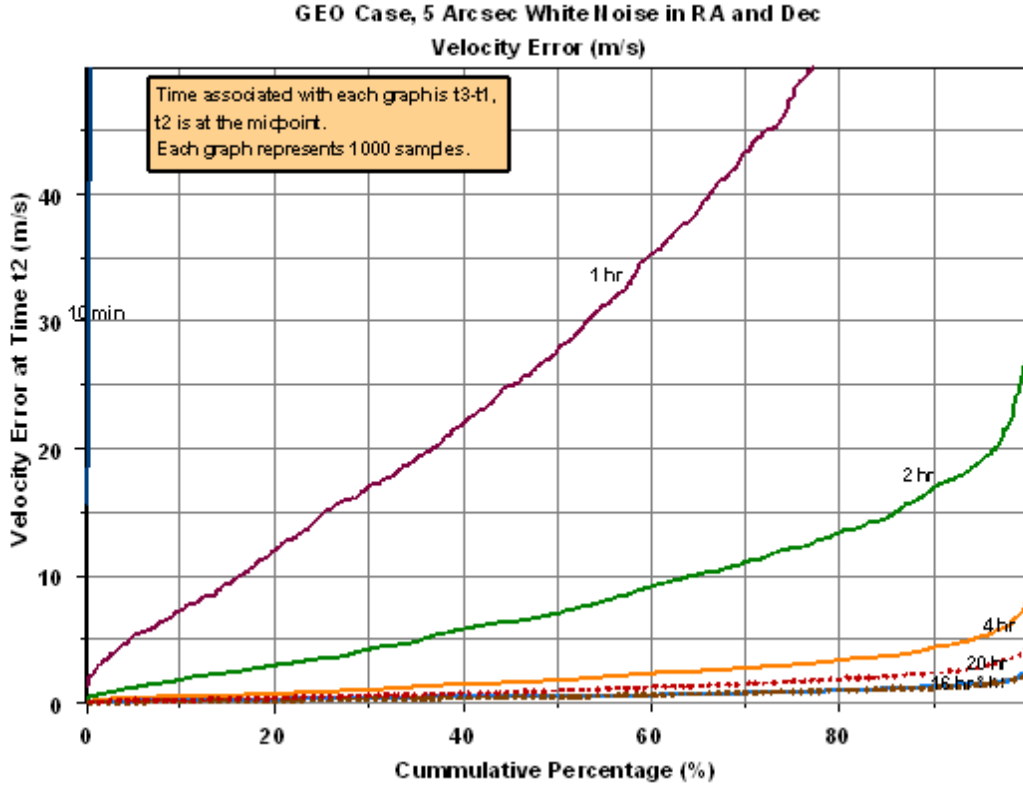


Figure 16: GEO Velocity Errors Single Station White Noise  $\sigma = 5$  arcsec

**LEO** Figs. 1 through 4 quantify and present position and velocity error root-sum-square (RSS) performance distribution graphics for single station subsets of right ascension and declination measurements. The RSS epoch is at  $t_2$ , centered in  $[t_1, t_3]$ . Input simulations used a white noise  $\sigma = 10$  arcsec for the first two graphs, and  $\sigma = 100$  arcsec for the last two graphs. For fixed white noise sigma, each graph presents  $(t_3 - t_1)$  parameterization functionals for  $(t_3 - t_1) \in \{(2), 4, 6, 8, 10\}$  min. A Monte Carlo ensemble of GoodingIOD solution experiments was defined, with ensemble size given in the graphic inset. Cumulative Percentage, presented on the abscissa, is a ratio multiplied by 100. The ratio denominator is Monte Carlo ensemble size. The numerator is the number of experiments for which the error RSS is less than the value defined by the associated ordinate. The ordinate for which the abscissa reads 100% is the RSS position error that captures the entire ensemble. For single station LEO measurements, conclude that the user of GoodingIOD should maximize the size of  $(t_3 - t_1) > 0$ .

Figs. 5 and 6 also present position and velocity error root-sum-square (RSS) performance distribution graphics for single station subsets of right ascension and declination measurements. For fixed  $(t_3 - t_1) = 8$  min, each graph presents white noise  $\sigma$  parameterization functionals for  $\sigma \in \{5, 10, 20, 50, 100\}$  arcsec. Conclude that the user of GoodingIOD should search for a measurement set such that  $(t_3 - t_1) \geq 8$  min. Conclude that the designer of receiver/antenna hardware should minimize his angles white noise Root-Mean-Square ( $RMS \approx \sigma$ ).

Figs. 7 and 8 quantify and present position and velocity error root-sum-square (RSS) performance graphics for *single-station* pairs of azimuth and elevation measurements due to measurement white noise samples from<sup>8</sup>  $\sigma = 0.01$  deg. The abscissa is defined by  $(t_3 - t_1) \in [1, 11]$  min. The position and velocity errors are huge.

<sup>8</sup>Note that  $0.01 \text{ deg} = 36 \text{ arcsec}$ .

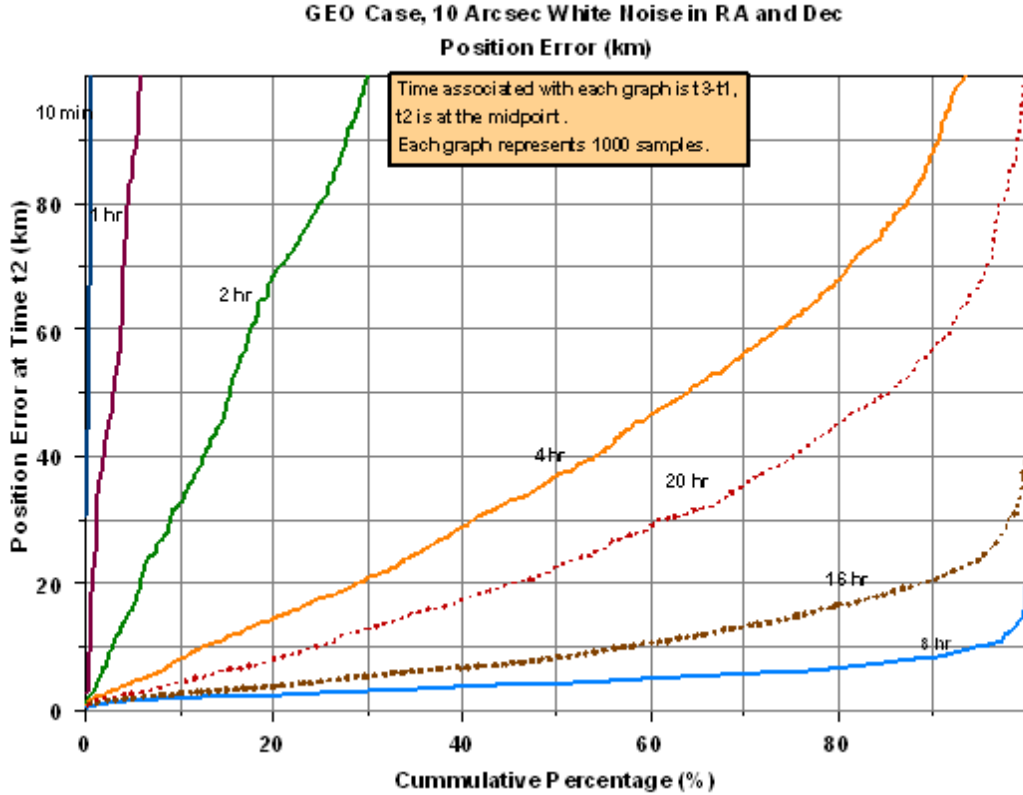


Figure 17: GEO Position Errors Single Station White Noise  $\sigma = 10$  arcsec

Figs. 9 and 10 quantify and present position and velocity error root-sum-square (RSS) performance graphics for *two-station* pairs of azimuth and elevation measurements due to measurement white noise samples from  $\sigma = 0.01$  deg. The abscissa is defined by  $(t_3 - t_1) \in [1, 50]$  min. Compare Figs. 9 and 10 with Figs. 7 and 8, and conclude that the user of GoodingIOD should prefer closely spaced *two-station* pairs of azimuth and elevation measurements to any combination of *single-station* pairs. Note that  $(t_3 - t_1) = 1$  min for each of the *two-station* pairs, and note that  $t_1$  for each of the two stations is contained within a six minute time interval; i.e., the time-tags of measurement pairs from the first station are close to those of measurement pairs from the second station.

Figs. 11 and 12 quantify and present position and velocity error root-sum-square (RSS) performance graphics for *two-station* pairs of azimuth and elevation measurements due to measurement white noise samples from  $\sigma = 0.01$  deg. The abscissa is defined by  $(t_3 - t_1) \in [1, 50]$  min. These figures are distinguished in that they reflect the use of full force model dynamics in the simulations. Compare Figs. 11 and 12 with Figs. 9 and 10. Conclude that accuracy performance is not significantly distinguishable.

**GEO** Figs. 13 through 16 quantify and present position and velocity error root-sum-square (RSS) performance distribution graphics for single station subsets of right ascension and declination measurements. Input simulations used a white noise  $\sigma = 2.5$  arcsec for the first two graphs, and  $\sigma = 5$  arcsec for the last two graphs. For fixed white noise sigma, each graph presents  $(t_3 - t_1)$  parameterization functionals for  $(t_3 - t_1) \in \{10 \text{ min}, 1 \text{ hr}, 2 \text{ hr}, 4 \text{ hr}, 8 \text{ hr}, 16 \text{ hr}, 20 \text{ hr}\}$ . Cumulative Percentage is presented on the abscissa. For single station GEO measurements, conclude that the user of GoodingIOD should select  $(t_3 - t_1) = 8 \text{ hr}$ . This is a surprising result!

Fig. 17 presents a position error root-sum-square (RSS) performance distribution graph for single station

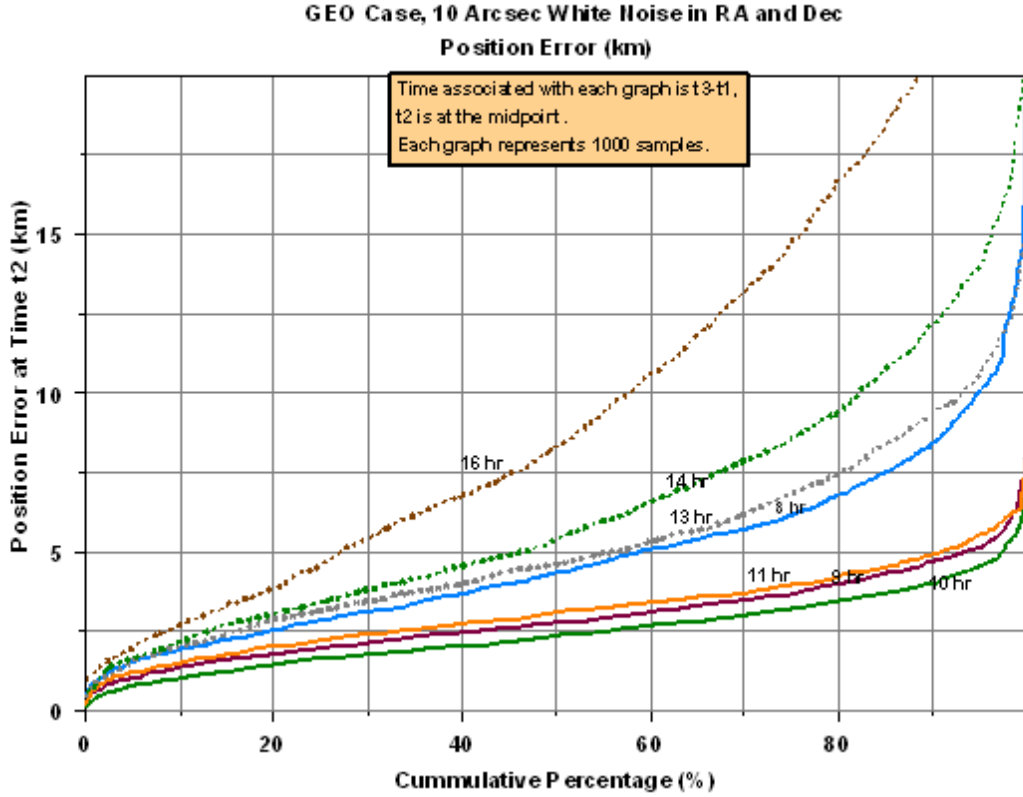


Figure 18: GEO Position Errors Single Station White Noise  $\sigma = 10$  arcsec

subsets of right ascension and declination measurements. Input simulations used a white noise  $\sigma = 10$  arcsec.

Figs. 18 and 19 present finer granularity in  $(t_3 - t_1)$  so as to look for a better case. Input simulations used a white noise  $\sigma = 10$  arcsec. Fig. 19 derives from two-station subsets. Conclude that the user of GoodingIOD should select  $(t_3 - t_1) = 10$ hr.

Compare Fig. 19 with Fig. 17 to conclude that two-station GoodingIOD is superior to single-station GoodingIOD.

## 5 Notation and Definitions

### 5.1 Notation

Use bold case symbols for vectors and non-bold case symbols for matrices and scalars. For time  $t_j$ ,  $j \in \{1, 2, 3\}$ :

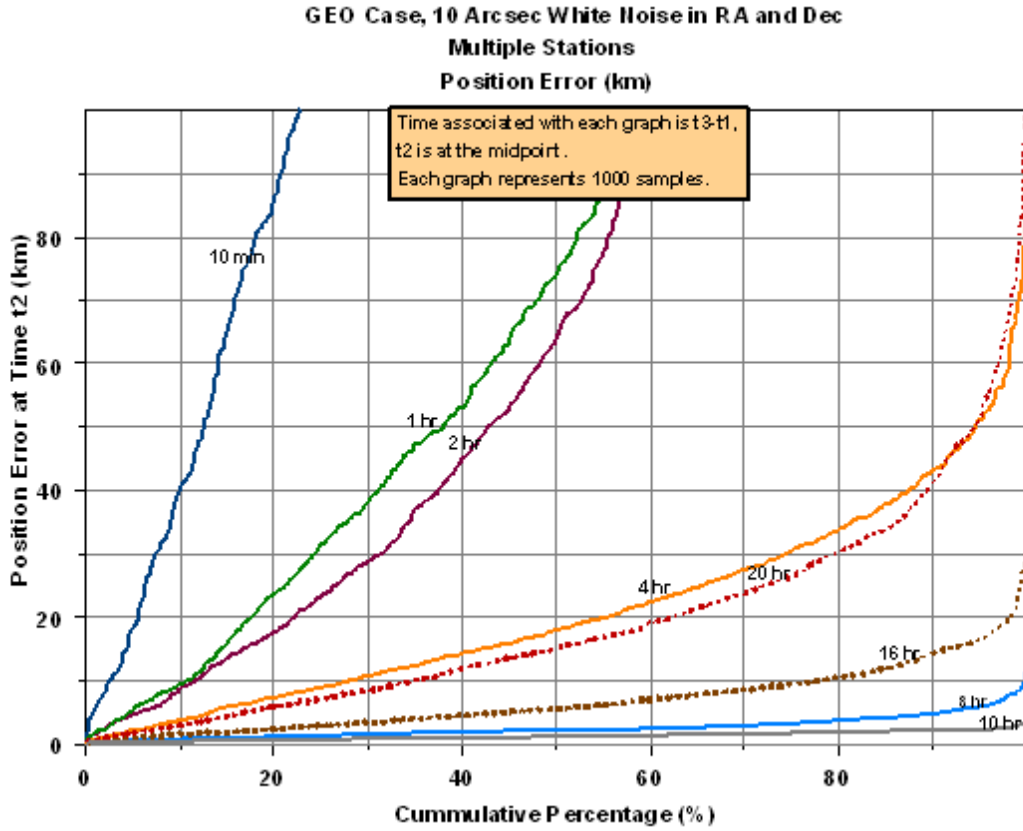


Figure 19: GEO Position Errors Multiple Station White Noise  $\sigma = 10$  arcsec

Symbol	Description
$t_j$	time/date
$\mathbf{r}_j$	spacecraft position vector (Earth Centered (EC))
$\dot{\mathbf{r}}_j$	spacecraft velocity vector (inertial time derivative)
$\boldsymbol{\rho}_j$	instantaneous range vector
$\rho_j$	instantaneous range, range vector length
$\mathbf{L}_j$	unit range vector
$\mathbf{s}_j$	ground station position vectors
$\alpha_j$	right ascension measurement
$\delta_j$	declination measurement
$\zeta_j$	azimuth
$\eta_j$	elevation

Table 3: Notation for Three Times

For any common time:

Symbol	Description
$\mu$	two-particle gravitational constant
$a$	semi-major axis
$e$	eccentricity
$i$	inclination
$\Omega$	node
$\omega$	argument of perigee
$\tau$	perigee time

Table 4: Notation for Any Common Time

## 5.2 Definitions

- $\boldsymbol{\rho}_j = \mathbf{r}_j - \mathbf{s}_j$ ,  $j \in \{1, 2, 3\}$
- $\rho_j = \sqrt{\boldsymbol{\rho}_j \cdot \boldsymbol{\rho}_j}$ ,  $j \in \{1, 2, 3\}$
- $\rho_1^{(0)}$  and  $\rho_3^{(0)}$  are initial range estimates (or guesses) for times  $t_1$  and  $t_3$
- $\mathbf{L}_j = \boldsymbol{\rho}_j / \rho_j$ ,  $j \in \{1, 2, 3\}$
- $\theta$  is central angle between satellite position vectors  $\mathbf{r}_1$  and  $\mathbf{r}_3$ , where  $0 \leq \theta < \infty$
- $k \in \{0, 1, 2, 3, \dots\}$  is the number of half-orbits  $k\pi$  for which  $\theta$  is completely contained
- $i = 0$  if  $k \in \{0, 1\}$ , but  $i \in \{0, 1\}$  if  $k \geq 2$ . Integer  $i$  indicates which of two Lambert solutions are to be used, if there are two.

## 6 Acknowledgements

We appreciate the detailed reviews by Bob Gooding and Dick Hujsak.

## References

- [1] Gauss, K. F., A Translation of *Theoria Motus*, BOOK II, Third Section, pp249-273, Dover, New York, 1963, first published by Little, Brown and Company 1857
- [2] Gooding, R. H., *A New Procedure for Orbit Determination Based on Three Lines of Sight (Angles Only)*, Technical Report 93004, Defence Research Agency, Farnborough, Hampshire, April 1993
- [3] Gooding, R. H., *A New Procedure for the Solution of the Classical Problem of Minimal Orbit Determination from Three Lines of Sight*, Cel. Mech. 66, 387 - 423, Kluwer Academic Publishers, 1997
- [4] Gooding, R. H., *On the Solution of Lambert's Orbital Boundary-Value Problem*, Technical Report 88027, Royal Aerospace Establishment, Farnborough, Hants, April 1988
- [5] Gooding, R. H., *A Procedure for the Solution of Lambert's Orbital Boundary-Value Problem*, Cel. Mech. 48, 145-165, Kluwer Academic Publishers, 1990
- [6] Wright, J. R., *ODTK Math. Spec.*, Analytical Graphics, Inc., 2004